

Stochastic Sampling Design using Multiobjective Genetic Algorithm and Adaptive Neural Networks

Kourosh Behzadian^a, Zoran Kapelan^{b,*}, Dragan Savic^b Abdollah Ardeshir^a

^a Department of Civil and Environmental Engineering, Amirkabir University of Technology, 424, Hafez Ave.- P.O. Box: 15875-4413- Tehran, Iran

^b Centre for Water Systems, University of Exeter, Harrison Building, North Park Road, EX4 4QF, Exeter, United Kingdom

ABSTRACT

This paper presents a novel multiobjective genetic algorithm (MOGA) based on NSGA-II algorithm, which uses metamodels to determine optimal sampling locations for installing pressure loggers in a water distribution system (WDS) when parameter uncertainty is considered. The new algorithm combines the multiobjective genetic algorithm with adaptive neural networks (MOGA-ANN) to locate pressure loggers. The purpose of pressure logger installation is to collect data for hydraulic model calibration. Sampling design is formulated as a two-objective optimization problem in this study. The objectives are to maximize the calibrated model accuracy and to minimize the number of sampling devices as a surrogate of sampling design cost. Calibrated model accuracy is defined as the average of normalized traces of model prediction covariance matrices, each of which is constructed from a randomly generated sampling set of calibration parameter values. This method of calculating model accuracy is called the ‘full’ fitness model. Within the genetic algorithm search process, the full fitness model is progressively replaced with the periodically (re)trained adaptive neural network

* Corresponding author. Tel: +44 1392 1392 264054; Fax: +44 1392 217965.

E-mail address: z.kapelan@exeter.ac.uk

meta-model where (re)training is done using the data collected by calling the full model. The methodology was first tested on a hypothetical (benchmark) problem to configure the setting requirement. Then the model was applied to a real case study. The results show that significant computational savings can be achieved by using the MOGA-ANN when compared to the approach where MOGA is linked to the full fitness model. When applied to the real case study, optimal solutions identified by MOGA-ANN are obtained 25 times faster than those identified by the full model without significant decrease in the accuracy of the final solution.

Keywords: Water distribution system; calibration; uncertainty; multiobjective genetic algorithm; adaptive neural networks.

INTRODUCTION

Data for the calibration of a water distribution system (WDS) model is usually collected from a series of field tests at strategic locations within the network in which the pressure head is recorded (de Schaetzen et al. 2000). The accuracy of calibration depends on the quality and quantity of the collected data. Therefore, the selection of appropriate collection locations, called the sampling design (SD), has been a challenge for researchers and practitioners (Kapelan et al 2005a).

Practitioners often use a simplified approach for sampling design since they seek straightforward applicable methods without the need for complex computations (Walski 1983). Although these methods are simple to understand and apply, they suffer from the lack of accuracy since they may require a logger to be located on nodes where pressures are insensitive with respect to calibration parameters. This way, the measurement locations that can return most of the information about calibration parameters may be easily omitted.

The above problem was overcome in the past by identifying sampling designs that have the optimal trade-off between calibrated model accuracy and the sampling design cost (Meier and Barkdoll 2000; de Schaetzen et al. 2000; Kapelan et al. 2003; Vitkovsky et al. 2003). However, all these models require estimating the calibration parameter values prior to the optimisation-based sampling design process. This is difficult to achieve as these values can be obtained accurately only after the model calibration.

To overcome this problem, a stochastic sampling design problem is formulated and solved here. The problem is formulated as an optimisation problem trading off the calibrated model accuracy with the sampling design cost but this time, calibration parameter values are assumed uncertain and modelled by using probability density functions. This way, a more realistic representation of the (essentially unknown) calibration parameter values is obtained which should lead to more robust sampling designs obtained. However, this comes at the price as stochastic sampling design problem is more difficult to solve than the deterministic one.

In this paper, an overview of sampling design and metamodeling approaches is briefly presented first. Optimal sampling design problem is then formulated. Following this, the methodology of the proposed algorithm, i.e. the multi-objective genetic algorithm and the adaptive neural network (MOGA-ANN), is described. The MOGA-ANN for SD is first tested on a hypothetical WDS, which is often used as a benchmark problem (Farmani et al., 2003), and then it is applied to a real case study. Finally, the relevant conclusions are drawn.

BACKGROUND

Sampling Design

The problem of sampling design for WDS models has attracted the attention of a number of researchers in recent years (Kapelán, 2002; Lansey, 2006). Only a few recently developed studies related to the proposed model are discussed here. A comprehensive overview of the relevant works can be found in Kapelán (2002).

Most of the developed SD approaches have been based on the sensitivity criteria of measurement locations with respect to calibration parameters. Mainly, Jacobian matrix and covariance matrix are used to find the most sensitive locations for monitoring (Yu and Powell 1994; Bush and Uber 1998; Lansey et al. 2001; Kapelán et al. 2003). These criteria have been used either to rank potential locations based on a sensitivity-based method (Ferreri et al. 1994; Bush and Uber 1998; Piller et al. 1999) or to create an optimization problem (Lee and Deiningger 1992; Meier and Barkdoll 2000; de Schaetzen et al. 2000; Kapelán et al. 2003; Vitkovsky et al. 2003).

In the ranking approach, a new measurement location with the highest sensitivity is added to the previously selected set of logger locations until the maximum number of loggers is reached. Clearly, such an approach will ignore the effect of all required measurement locations simultaneously. However, when compared to the empirical methods, the sensitivity-based approach is far superior, and yet easy to apply without solving a complex optimization problem.

The optimization model can take into account the effect of a set of monitoring locations altogether and their mutual interactions when performing SD for a set of specified monitoring locations. Most

SD approaches have used genetic algorithms (GAs) to solve the associated optimization problem (Meier and Barkdoll 2000; de Schaetzen et al. 2000; Kapelan et al. 2003; Vitkovsky et al. 2003).

Bush and Uber (1998) proposed three sensitivity-based methods to rank the locations of pressure and tracer measurements within WDS for model calibration. All three methods are based on minimizing the uncertainty in estimated parameter values (directly or indirectly). Lansey et al. (2001) developed an SD procedure based on a three-step calibration process to consider the uncertainties in measurement and estimation. The trace of the model prediction covariance matrix is used as the model uncertainty. They finally proposed how to identify the preferable conditions and locations for data collection based on the uncertainty and sensitivity-based heuristic analysis.

The model by Kapelan et al. (2003) presented a deterministic multi-objective genetic algorithm (MOGA) for SD prior to WDS model calibration. The two objectives proposed were to maximize calibrated model accuracy and to minimize total SD costs. The authors also proposed and compared three different approaches for evaluating the model accuracy, which were calculated using some norms of the parameter itself or the prediction covariance matrix. In this approach, elements of the Jacobian matrix are calculated prior to the optimization model run by assuming the model parameter values. This approach is obviously prone to errors as that kind of information is not readily available when measurement locations are being selected.

In water quality management, optimal sensor placement in WDS has also attracted special attention with the aim of identifying contamination sources (Ostfeld and Salomons 2004; Berry et al. 2005; Propato, 2006; Berry et al. 2006; Shastri1 and Diwekar 2006). They all typically minimize the risk from contamination using sensors for timely detection.

Meta-modelling

The use of metamodels to reduce the computational times in optimisation processes was proposed by Blanning (1975). A metamodel can be used as a surrogate for calculating fitness values, which are normally based on time-consuming simulations. Such a metamodel can be effectively integrated into the search process to gradually substitute the large portion of simulation which model runs require. One of the frequently used metamodels is the artificial neural network (ANN) because of its ability to approximate effectively a wide range of nonlinear functions (Leshno et al. 1993).

Historically, ANNs have been successfully applied to several water resource problems, such as groundwater remediation designs (Rizzo and Dougherty 1996; Rogers et al. 1995; Aly and Peralta 1999; Yan and Minsker 2005). In a recently developed application, Yan and Minsker (2006) reported a model for groundwater remediation design that makes use of an adaptive neural network and a single objective genetic algorithm. They saved approximately 90 percent of the simulation model calls with no loss in accuracy in the optimal solutions. In the context of water distribution systems, a few applications using ANNs have been observed. Lingireddy and Ormsbee (1998) applied ANNs to optimal calibration of a WDS model. Recently, Broad et al. (2005) proposed ANNs as a substitution for a complex simulation model for WDS design, in which ANNs were trained offline. As ANNs were trained before being used by the optimization model, the authors proposed setting some heuristic rules to prohibit solutions becoming infeasible.

OPTIMAL SAMPLING DESIGN

The objective of the SD here is to find a set of optimal measurement locations with the aim of calibrating accurately the WDS hydraulic model. The stochastic SD problem is formulated and

solved as a two objective optimization problem under parameter uncertainty. The two objectives are the maximisation of the calibrated model accuracy and the minimisation of the sampling design cost.

To quantify the calibrated model prediction accuracy, a first-order second-moment (FOSM) model is used to approximate the relevant parameter and prediction covariance matrices. Without the loss of generality, it is assumed that prediction and measurement variables of interest are nodal pressures only. As a consequence, if a set of N_l measurement devices with the standard deviation of s are installed in N_l measurement WDS locations, the variance of calibrated parameters can be estimated from the diagonal elements of the parameter covariance matrix (Bush and Uber 1998, Kapelan et al. 2005a):

$$\mathbf{Cov}_a = s^2 \cdot (\mathbf{J}^T \mathbf{J})^{-1} \quad (1)$$

where \mathbf{J} =Jacobian matrix of derivatives $\partial y_i / \partial a_k$ ($i = 1, \dots, N_o; k = 1, \dots, N_a$), y =vector of N_o pressure predictions at locations where loggers are installed, a =vector of N_a calibration parameters, N_o =number of observations, i.e. measurement data in both spatial and temporal domains (e.g. if there are N_t time steps for each of N_l monitoring locations, then $N_o = N_t \cdot N_l$), N_a =number of calibration parameters.

The uncertainty in model predictions (e.g. pressures) at any location in the system can be estimated from the diagonal elements of the prediction covariance matrix (Lansey et al. 2001, Kapelan et al. 2005a):

$$\mathbf{Cov}_z = \mathbf{J}_z \cdot \mathbf{Cov}_a \cdot \mathbf{J}_z^T \quad (2)$$

where \mathbf{J}_z =Jacobian matrix of derivatives $\partial z_i / \partial a_k$ ($i = 1, \dots, N_z; k = 1, \dots, N_a$); z =vector of N_z pressure predictions of interest. Note that there are several general methods for the calculation of elements of the Jacobian matrices \mathbf{J} and \mathbf{J}_z (Kapelan et al. 2003).

To aggregate the model prediction uncertainty, the average of square root of all diagonal elements in matrix \mathbf{Cov}_z (i.e. standard deviations of model predictions) is assumed as the model uncertainty:

$$f_1 = \frac{1}{N_z} \sum_{i=1}^{N_z} \mathbf{Cov}_{z,ii}^{1/2} \quad (3)$$

Therefore, the normalised prediction accuracy is then defined as follows (Kapelan et al. 2003; Bush and Uber 1998):

$$F_1 = \frac{f_{1,ml}}{f_1} \quad (4)$$

where $f_{1,ml}$ =the value of model uncertainty for the ideal state where all potential measurement locations are monitored. Note that if model uncertainty (equation 3) is to be minimised then normalized prediction accuracy (equation 4) has to be maximised.

Note that all N_a calibration parameters have to be assigned a value before the values of the full Jacobian matrix can be calculated, i.e. before sampling design process can commence. These values, however, are not normally available prior to the sampling design process. To overcome this problem, each calibration parameter is assumed here to be uncertain following some pre-defined probability density function (PDF). It is envisaged that this should enable a more realistic representation of essentially unknown calibration parameter values.

As a consequence, the calibration accuracy objective is defined here as the average of normalised prediction accuracies (see equation (4)), each of which is constructed from a randomly generated sample of calibration parameter values:

$$\text{Maximise } F_1 = \frac{1}{N_k} \sum_{j=1}^{N_k} \frac{f_{1,ml}^j}{f_1^j} \quad (5)$$

where N_k = number of sets of samples and superscript j refers to j th sampling set. This approach to calculating the first objective value is called the ‘full’ fitness model henceforth. To do so, N_k sets of uncertain parameter values are randomly generated from the associated PDFs by using the Latin Hypercube (LH) sampling technique (McKay et al. 1979, Helton and Davis 2003). The noisy objective value is then calculated by averaging the relative accuracies obtained by N_k runs of the deterministic SD model.

The sampling design cost is surrogated by the number of devices used leading to the following second optimisation objective and the associated constraint:

$$\text{Minimise } F_2 = N_l / N_{ml} \quad (6)$$

$$N_l^{\min} \leq N_l \leq N_l^{\max} \quad (7)$$

where N_{ml} = number of potential measurement locations; N_l^{\min} , N_l^{\max} = minimum and maximum number of measurement devices used, respectively.

METHODOLOGY

The objectives and the constraints shown in equations (5)-(7) define a two-objective optimisation problem under uncertainty. The main problem here is how to efficiently calculate the value of first objective function (see equation (5)) due to the time consuming nature of repetitive Jacobian matrix calculations. To resolve this, the optimisation problem is solved by using the multi-objective genetic algorithm coupled with adaptive neural networks (MOGA-ANN).

Each GA chromosome is coded as a potential sampling design solution and its fitness is evaluated initially by using the full fitness model (i.e. with a number of samples). Later on, during the GA search process, the full fitness model is progressively replaced with the periodically (re)trained ANN metamodel where (re)training is done using the data collected from the previous evaluations by the full model. The ANN is retrained after a pre-specified number of objective function evaluations using the full model. The detailed flowchart of MOGA-ANN is shown in Figure 1.

Multi-objective Genetic Algorithm

Here, a multi-objective evolutionary algorithm known as the Non-dominated Sorting Genetic Algorithm II (NSGA-II) is used (Deb et al., 2002). NSGA-II alleviates all of the following difficulties of previous MOGAs: (1) considerable computational effort, (2) non-elitism approach, (3) the need for the specification of a sharing parameter. The selection operator in NSGA-II combines the parent and offspring populations in a single population and then selects the best solutions with respect to fitness and spread criteria. More details of this approach can be found in Deb et al. (2002).

Integer value coding is used for the encoding of each chromosome. The number of genes equals the maximum number of measurement devices (N_l^{\max}), each of which represents the position of one pressure logger in WDS. A gene with zero value indicates no measurement device is available. When using integer encoding, two or more genes may take the same integer value, indicating more than one pressure logger should be installed in the same location. These solutions will be rejected by MOGA due to an increase in cost and no increase in accuracy (Kapelan 2002).

Artificial Neural Network (ANN)

The ANN is used here as a replacement for a full fitness evaluation model used when estimating the model accuracy objective with the idea of making significant computational time savings. However, ANN predictions are only approximate and, therefore, prone to errors when used to evaluate the objective value. To resolve this problem, several strategies have been proposed to sample solutions and calculate the relevant objective value with the full model. In addition, the ANNs are periodically retrained within the algorithm progress to improve their prediction accuracy.

Figure 2 shows the architecture of the proposed ANN. As it can be seen, a conventional neural network with an input, hidden and an output layer is assumed. Input data are defined as

measurement locations, hence the number of input layer neurons is equal to the maximum number of measurement devices (See above). The output layer has one neuron only equal to the value of first objective function (prediction accuracy), as defined in equation (5). The second objective function value, i.e. the number of measurement locations, is directly calculated and there is no need to consider it as an additional output neuron. The back propagation Levenberg-Marquardt algorithm is used to train the ANN (Lingireddy and Ormsbee 1998).

MOGA-ANN Algorithm

A flowchart of the proposed MOGA-ANN method is shown in Figure 1. It can be seen that the method is essentially a modified NSGAII algorithm that makes use of the ANN and the caching technique. The search process starts by creating a random initial population and evaluating the fitness of each chromosome by using the full fitness evaluation model. The data obtained (both chromosome components, i.e. genes and relevant objective function values) is then stored in the cache with the idea of preventing costly repetitive fitness evaluations. The cache is updated continuously during the search process, i.e. every time chromosome fitness is evaluated using the full model.

The main loop of the algorithm starts with the creation of the offspring population using the NSGA-II selection, crossover, and mutation operators. In the first few generations, chromosome fitness is estimated using the full model only, in order to collect enough ANN training data (steps 5-7 in Figure 1). Once the ANN is trained for the first time, evaluation of objective function values is done by using both ANN and the full model (steps 10-13 in Figure 1). At first, objective values of all chromosomes in the offspring population are evaluated by using the ANN. Then the offspring chromosomes are compared to the ones previously stored in the cache. If the offspring chromosome

is found in the cache then its accuracy objective value (approximated by the ANN) is replaced with the corresponding value from the cache (estimated previously by the full model).

To improve the algorithm convergence, a (small) number of chromosomes in the offspring population is selected and re-evaluated by using the full model (if they were previously evaluated by the ANN). The chromosomes selected are the ones present in the best NF Pareto (sub)fronts, i.e. subpopulations of the offspring population.

Furthermore, when using the integer coding, two or more genes in a newly created chromosome may have the same value indicating that more than one pressure logger should be placed on the same network node, i.e. indicating an infeasible solution. Even though they should be rejected, such chromosomes are considered by the MOGA-ANN model because of the errors in ANN predictions and, as a consequence, these solutions may still appear in the best NF Pareto (sub)fronts. Although applying the above re-evaluation would cause such infeasible solutions to be rejected quickly, it would lead to a weak convergence of the algorithm. To avoid this, a penalty is added to the accuracy objective function value of these chromosomes.

Once the offspring population is created by using the above procedure, it is combined with the parent population into a single one. The next generation population is then created by using the standard NSGA-II approach. At this point an additional check is made and if a chromosome fitness value is estimated by the ANN, its fitness is re-evaluated by using the full model. This is necessary to ensure good algorithm convergence and it typically involves a small number of chromosomes. The above search process continues until some convergence criterion is met.

In addition to standard NSGA-II parameters, MOGA-ANN has some additional parameters which have to be set before performing the optimisation run. This includes setting the values of: NF , the number of Initial Training Generations (ITG), the number of retraining data and the number of neurons in a hidden layer. The MOGA-ANN is first rigorously analysed in a hypothetical case study to identify the optimal MOGA-ANN model parameter values. These parameter values are then used in a real case study.

Best ranked Pareto-(sub)fronts (subpopulations). As noted above, after identifying all Pareto sub-fronts in the offspring population, members of the best NF fronts are checked to see whether their fitness has been calculated by the full model. If not, they are re-calculated using the full model. Obviously, a trade-off exists here - the larger the NF the better results are achieved from the search accuracy point of view, but worse from the computational time point of view.

Number of initial training generations (ITG). A number of initial full model fitness evaluations are required to obtain data for the first ANN training. This data is collected by using the full fitness model only when evaluating chromosomes in the first ITG generations. A sensitivity analysis is performed to determine the minimum number of ITG required for the good MOGA-ANN performance.

Number of retraining data. To increase the accuracy of ANN predictions, ANNs need to be periodically retrained with new data. The number of retraining data points is defined as the number of additional (i.e. new) full fitness model evaluations that is collected before ANN is (re)trained. There are two possible approaches for collecting additional training data (Yan and Minsker 2006): (1) the growing set approach and (2) the fixed set approach. In the former approach, the ANN

retraining is accomplished with both new and existing data (each time the ANN is retrained) whilst in the latter approach existing data are replaced with new data (leading to the constant number of retraining data and hence, smaller data sets than in the growing set approach). Thus, the fixed set approach typically needs less time for retraining and contains less data but may lead to lower prediction accuracy. A novel mix of the above two approaches is adopted here to exploit the benefits of both. The growing set approach is used first to gather (re)training data until some predefined data capacity is reached. After this, new data are replaced with the oldest existing data which are less likely to be found by the genetic algorithm search.

CASE STUDIES

Case #1: Literature Example

The above methodology is first tested and verified on a literature benchmark case study of the Anytown network (Kapelan et al 2003, Ormsbee 1989). The objective is to test and verify the computational efficiency and accuracy of the proposed MOGA-ANN method. The comparison is made between the MOGA-ANN model and the MOGA model (the latter being based on full fitness evaluations only, i.e. no use of either ANN nor caching).

Figure 3 shows the layout of the Anytown network. The network configuration data has been taken from Ormsbee (1989). Sampling design is performed with respect to 5 grouped pipe roughness coefficients and 4 grouped nodal demands ($N_a=9$). All network nodes are considered as potential pressure measurement locations except for the reservoir and tank nodes ($N_{ml}=16$). Full Jacobian matrix \mathbf{J}_{ml} is obtained by using all potential measurement locations and loading conditions leading to $N_o=128$ (16 nodes for 8 steady-state loading conditions). The standard deviation of all pressure

loggers is assumed to be equal to $s=0.1$ m. The value of N_k is set to 200 samples which is sufficient for the noisy function based on the sensitivity analysis performed (not shown here). The following assumptions are made about uncertain parameters: (1) uncertain pipe roughness coefficient parameters follow a uniform PDF with lower and upper bounds equal to $\pm 30\%$ of the deterministic value; (2) uncertain nodal demand parameters follow a Gaussian PDF with coefficient of variation (CV) equal to 0.20.

GA parameters were determined after a limited number of trial runs with different initial populations. The following parameters are used here: population size of 50, binary tournament selection operator, random-by-gene mutation with the probability of 0.25 and single-point crossover with the probability of 0.90. All MOGA and MOGA-ANN runs were performed for 500 generations.

MOGA-ANN algorithm parameters were determined by the sensitivity analyses. The criteria for comparing different sets of parameter values are the number of full fitness evaluations and the search model reliability. The latter is denoted here as the percentage of Pareto optimal front points obtained by using the MOGA-ANN model when compared to the MOGA model. This percentage has been averaged over 20 MOGA runs with different random initial populations. The number of best ranked Pareto-(sub)fronts (NF) is examined especially since it has a major effect on both comparison criteria.

Figure 4 shows the average number of full model evaluations for three values of NF and ITG . As it can be seen, when the NF is increased, the average number of full model evaluations increases monotonically, and yet, considerably compared to the increasing ITG . Figure 5 shows the model

reliability sensitivity with respect to the two MOGA-ANN parameters. Based on this figure the best MOGA-ANN performance is achieved for $ITG=6$ and $NF=2$ or 3.

Figure 6 shows the sensitivity of model reliability to the number of retraining data. As it can be seen, for $NF=1$ and 2, model reliability decreases when the number of retraining data increases. This decrease for $NF=1$ is about 10% when the number of retraining data is increased from 1000 to 2000 because ANNs are not updated after their first training. However, the same decrease in model reliability is much lower for $NF=2$ because ANNs are re-trained during the search process and hence the required training data for $NF=2$ is obtained earlier than the corresponding data for $NF=1$. For $NF=3$, model reliability is not dependent on the number of retraining data (always 100%) showing that the value of $NF=3$ is large enough to cover all errors arising from different ANN updating.

Figure 7 shows the sensitivity of model reliability to the number of neurons in ANN's hidden layer. As can be seen, model reliability of 100% is obtained for $NF=2$ and the number of neurons equal to 20 and 30 and $NF=3$ (regardless of the number of hidden layer neurons). Since a larger number of hidden neurons would lead to longer ANN training times, the number of hidden layer neurons equal to 20 is selected here.

Based on the above sensitivity analyses, the following MOGA-ANN specific parameter values are used here: $ITG=6$, $NF=3$, number of ANN hidden layer neurons = 20 and ANN re-training every 1000 full model fitness evaluations.

To validate and compare the results (i.e. the optimal sampling locations) obtained by using the MOGA-ANN model, the Monte Carlo Simulation (MCS) based model is developed and used here.

In the MCS-based model, an equivalent deterministic sampling design optimization problem (i.e. maximization of normalized prediction accuracy defined by equation (4)) is solved for a number of randomly generated calibration parameter samples. Optimal sampling locations are then determined by identifying the most frequently selected sampling locations in these optimization runs. Based on the separate sensitivity analysis performed (not shown here), 200 samples were deemed sufficient for the MCS model.

The optimal sampling locations obtained by the MOGA-ANN model are shown in Table 1. The table also shows the percentage of selected sampling locations obtained by the MCS-based model. As it can be seen, the most frequently selected sampling locations in the MCS-based model (framed fields) almost always correspond to the optimal ones determined by the MOGA-ANN model. Of course, some discrepancies exist too (dark coloured fields). The differences occur inevitably due to the different approaches used in the two methods when dealing with uncertainty. Nevertheless, 93% of solutions matched show similarity in the results obtained using the above two stochastic approaches. Note that the MOGA model found the same solutions as the MOGA-ANN model and hence its optimal measurement locations are not shown in Table 1.

When comparing the percentage of optimal measurement locations obtained by the MCS-based model in Table 1, it can be observed that the average percentage for a few sampling locations is not as robust as the one for a large number of sampling locations. For example, the average of these percentages for four optimal measurement locations is 64% whilst the same value for eight optimal measurement locations is 89%. This implies that a small set of optimal measurement locations have more uncertainty than a large set of measurement locations under stochastic sampling design.

Furthermore, for each given number of monitoring devices in Table 1, a relatively uniform distribution of optimal measurement locations is seen within the network. This can be interpreted as the tendency of the model to cover all parts of the network. However, these devices are usually located in places far from transmission pipes which are often close to main sources. For example, nodes 20 and 30, which connect the main source and the main costumers, consistently rank low. On the other hand, nodes which are the final receivers of water are the most sensitive nodes and hence they can be the first candidates for selection. For example, the flow in all connecting pipes linked to nodes 90, 120 and 170 are almost always directed towards these nodes, which indicates that they do not transmit water. This can be because such nodes are the most sensitive ones with respect to the head loss changes. Nonetheless, other factors can affect the selection process of optimal locations such as the layout of the grouped calibration parameters, or the existence of the loop in the network.

To compare the Pareto optimal front obtained by the MOGA-ANN and the MCS-based models, solutions are further evaluated in the same uncertain environment. To do so, the following steps are preformed: (1) 10,000 sets of uncertain parameter values are randomly generated according to the pre-specified parameter PDFs; (2) for each model the normalised prediction accuracy (see equation (5)) is calculated for each optimal measurement location identified in the 10,000 samples.

Figure 8 shows Pareto optimal fronts obtained by the aforementioned method for the two stochastic models. The values of prediction accuracy of both models are also shown in the third column of Table 1. As can be seen from Figure 8, both Pareto optimal fronts match reasonably well although MOGA-ANN's front seems to be slightly better for a small numbers of measurement locations. Also, note that most the calibration accuracy is gained by installing 6-7 loggers. This fact could be used when selecting the 'best' solution from the Pareto front (Kapelan et al. 2005b).

To further compare solutions obtained by the MOGA-ANN and MCS-based models, the four optimal monitoring locations identified by each of these two methods are shown in Figure 3. Here it shows that three out of four monitoring locations are identical. The statistics of relative pressure prediction accuracy which resulted from model simulations in the uncertain environment are given in Table 2. It can be seen that both statistics are similar to each other.

Figure 9 shows the comparison of the number of the actual function evaluations using the full model, the caching technique and the ANN approximations as the MOGA-ANN model search progresses. It can be seen from this Figure that a total of 12% of chromosomes are evaluated by using the full fitness evaluation model. Most of these evaluations occur in the first six generations of the MOGA-ANN model when the initial ANN training data is obtained. After that, the proportion of the full model evaluations decreases in favour of two other means of estimating the solution fitness. The percentage of objective values retrieved from the cache is almost constant at 25% once the initial ANN training is done.

Table 3 shows the comparison of computational effort for the three aforementioned stochastic sampling design models. As can be seen from the second column of this table, the MOGA-ANN model achieves optimal solutions 8 times faster (87% savings) than the MOGA and the MCS-based models.

Case #2: Real-world Case Study

Here, the proposed MOGA-ANN sampling design model is further tested and verified on the Mahalat WDS shown in Figure 10. The city of Mahalat is located in the central part of Iran. The

WDS covers an area of approximately 46 km², with a population of around 160,000. The city is located on a steep slope with the lowest elevation of 1584 m.a.s.l. while the highest elevation is 1900 m.a.s.l. Water demands are predominantly domestic with some commercial users. To reduce the high pressure head induced by the steep slope, six pressure reducing valves (PRVs) are used to decrease pressure heads to pre-specified values. The total number of pipes defined in the original WDS is 1814 with the total length of approximately 101 kilometres.

The dominant pipe materials (see Table 4) are ductile iron (larger pipe diameters), PVC (small diameter pipes) and asbestos cement (most of the middle diameter pipes). The skeletonised EPANET hydraulic model has 237 pipes, 195 junctions, 2 tanks and 6 PRVs. The WDS is supplied by gravity and pumped from three wells and two service tanks (reservoirs). The position of the water supply sources (two wells) is marked in Figure 10 as 'Inflow'. The third well supplies the two reservoirs. The average water demand in the network is 158.9 l/s.

It is assumed that the above WDS model will be calibrated for 7 grouped pipe roughness coefficients, i.e. $N_a=7$. Although there are a large number of pipes (237 pipes), the small number of calibration parameter groups is assumed to primarily keep the calibrated model prediction error low but also to reduce the computational effort (Mallick et al. 2002). The Hazen Williams (HW) pipe roughness coefficients were first grouped using engineering tables and proposed relationships based on the diameter, material, lining and age of pipes (Walski et al. 1988; Kapelan 2002). Then, the final pipe grouping was performed by dividing the range of identified HW pipe roughness coefficients (78-155) into the following groups: (78,90], (90,100], (100,110], (110,120], (120,130], (130,140] and (140,155]. Once this was done, the average value at each interval was considered as the group's representative roughness coefficient value. Furthermore, it was assumed that the Mahalat model

would be calibrated for normal demand loading condition only. The standard deviation of all pressure loggers was assumed equal to $s=1.0$ m.

Since the number of calibration parameters is equal to 7 ($N_a=7$), the constraint on the minimum number of measurement devices (N_{min}) is set to 7. This ensures that the sampling design solution will lead to at least an even-determined calibration problem. Furthermore, each node of the network was considered as a potential measurement location ($N_{nl}=195$). However, the maximum number of 50 measurements ($N_{max}=50$) was introduced as the SD budget limit.

MOGA model settings were determined after a limited number of trial runs with different initial populations. The following settings have been used for GA parameters in all model runs: population size of 200, binary tournament selection, random-by-gene mutation with probability rate of 0.05 and single point crossover with probability rate of 0.80. All MOGA runs were performed for 8,000 generations. The additional MOGA-ANN model parameters were set equal to the values obtained in the first case study. When compared to this case study, the maximum training data capacity needs to be defined in this case because of the large number of full fitness evaluations. Therefore, the caching capacity of 5000 was assumed for the Mahalat case study. Furthermore, the following assumptions are made about uncertain parameters: (1) The calibration parameters are assumed to be only pipe roughness coefficients, all following a uniform PDF with lower and upper bounds equal to $\pm 30\%$ of the deterministic value; (2) uncertain nodal demands following a Gaussian PDF with coefficient of variation (CV) equal to 0.3 were modelled too (but not calibrated for).

The near optimal measurement locations are obtained by running both the MOGA and the MOGA-ANN models. As the lists of these sampling locations are long (between 7 and 50), only the Pareto

optimal fronts obtained are shown here. The same methodology used in case #1 is used here to compare the two Pareto optimal fronts.

Figure 11 shows the Pareto optimal fronts obtained by the MOGA and the MOGA-ANN models. The following can be observed: (1) both fronts match reasonably well although there is a minor advantage of MOGA over MOGA-ANN for the large number of monitoring locations. As a consequence, solutions obtained by the MOGA-ANN model represent a good surrogate of the solutions obtained by using the MOGA model; (2) An average normalized accuracy of approximately 60% is attainable by monitoring 25% optimal measurement locations (i.e. by using 50 pressure loggers); (3) The rate of increase in WDS model prediction accuracy declines quickly with the increase in number of monitoring locations; for example, adding one more measurement location when 4% locations are already monitored improves the normalized calibrated WDS model prediction accuracy by 3%, while adding one more sampling location when 10% of the system is monitored leads to an improvement (in normalised WDS model prediction accuracy) of less than 1%.

The ten MOGA-ANN and MOGA optimal monitoring locations are shown in Figure 10. Only four monitoring locations are identical although other monitoring nodes are relatively close to each other. The statistics of relative pressure prediction accuracy (equation 4) and pressure prediction uncertainty (equation 3) obtained by using the model simulation in the uncertain environment are given in Table 5. The 95% confidence interval for pressure prediction is between 0.18 and 0.27 in both models. The statistics show similar relevant objective values although the optimal monitoring nodes are not quite the same. This is probably due to the fact that as in many other large-size optimization problems, there are many combinations of near optimal solutions (i.e. monitoring

locations) that can produce similar fitness statistics. Figure 10 also shows that the distribution of ten optimal measurement devices is relatively uniform within the network. The selected measurement locations are usually located away from the main sources and transmission pipes. This confirms that the optimal measurement locations satisfy suggestions put forward by Walski (1983) and verified by Kapelan et al. (2003).

Table 6 shows the comparison of computational times for the two stochastic SD models. It can be seen in the case of a real world problem, that the main advantage of the MOGA-ANN model when compared to the MOGA model, is that Pareto optimal solutions are obtained with large computational savings (96% approximately) without significant decrease in accuracy.

Finally, Figure 12 shows the proportion of different types of fitness evaluations performed by the MOGA-ANN model in the case of the Mahalat WDS. This Figure shows that less than 1% of all fitness evaluations are performed by using the full model, 65% are performed by using the ANN and the rest is obtained by using the caching technique.

SUMMARY AND CONCLUSIONS

This paper addresses the problem of stochastic WDS sampling design for calibration. The objective is to identify best measurement locations in the WDS that should be used to collect the relevant data for subsequent model calibration. The sampling design is formulated and solved as a two-objective optimisation problem under calibration parameter uncertainty. The two objectives are the maximisation of the calibrated model accuracy and the minimisation of the number of sampling

devices used (used as a surrogate for sampling design cost). Uncertain calibration parameters are characterised by means of pre-specified PDFs.

The sampling design problem is solved by the new MOGA-ANN algorithm. This is a modified NSGA-II algorithm, which makes use of artificial neural networks and the caching technique to reduce the computational burden. The periodically retrained ANNs are used as surrogate models during the optimisation process to speed up the fitness evaluations. The caching technique is used to retrieve previously evaluated solutions efficiently and prevent re-evaluation.

The MOGA-ANN algorithm is tested and verified on two case studies, the benchmark problem of a hypothetical network (Anytown), and the real case study of the Mahalat WDS. The results obtained clearly demonstrate that substantial computational savings can be achieved by using the MOGA-ANN model without significant loss of accuracy. This is a promising result when it comes to solving stochastic sampling design or generally time-consuming multiobjective optimization problems for large-scale WDSs. Having said this, further research work is required to test and verify the capability of the proposed approach before achieving that goal. In addition, improvements achieved by stochastic sampling design should be further investigated in real case studies.

REFERENCES

- Aly, A.H., Peralta R.C., 1999. Optimal design of aquifer cleanup systems under uncertainty using a neural network and a genetic algorithm. *Water Resources Research* 35(8) 2523– 2532.
- Blanning, R.W., 1975. The construction and implementation of metamodels. *Simulation* 24(6) 177– 184.

- Berry, J.W., Fleischer, L., Hart, W.E., Phillips, C.A., Watson, J.P., 2005. Sensor placement in municipal water networks. *Journal of Water Resources Planning and Management* 131(3) 237-243.
- Berry, J.W., Hart, W.E., Phillips, C.A., Uber, J.G., Watson, J.P., 2006. Sensor placement in municipal water networks with temporal integer programming models”, *Journal of Water Resources Planning and Management* 132(4) 218-224.
- Broad, D.R., Dandy, G.C., Maier, H.R. 2005. Water distribution system optimization using metamodels, *Journal of Water Resources Planning and Management* 131(3) 172-180.
- Bush, C.A., Uber, J.G., 1998. Sampling design methods for water distribution model calibration. *Journal of Water Resources Planning and Management* 124(6) 334-344.
- Deb, K., Pratap, A., Agarwal, S., Meyarivan, T., 2002. A fast and elitist multiobjective genetic algorithm: NSGA-II. *IEEE Trans. Evol. Comput.* 6(4) 182–197.
- de Schaetzen, W., Walters, G.A., Savic, D.A., 2000. Optimal sampling design for model calibration using shortest path, genetic and entropy algorithms. *Urban Water* 2 141–152.
- Farmani, R., Savic, D.A., Walters, G.A., 2003. Benchmark problems for design and optimisation of water distribution systems, *Advances in Water Supply Management*, Maksimovic, C., D. Butler and F. Memon (eds.), A.A. Balkema Publishers, pp. 249-256.
- Helton, J.C., Davis, F.J., 2003. Latin hypercube sampling and the propagation of uncertainty in analyses of complex systems. *Reliability Engineering and System Safety* 81, 23-69.
- Kapelan, Z., 2002. Calibration of WDS hydraulic models. PhD thesis, School of engineering and computer science, Univ. of Exeter, Exeter, U.K.
- Kapelan, Z., Savic, D.A., Walters G.A, 2003. Multi-objective sampling design for water distribution model calibration. *Journal of Water Resources Planning and Management* 129(6) 466-479.

- Kapelan, Z., Savic, D.A., Walters G.A. 2005a. Optimal sampling design methodologies for water distribution model calibration. *Journal of Hydraulic Engineering* 131(3) 190-200.
- Kapelan, Z., Savic, D.A., Walters, G.A., 2005b. Multiobjective design of water distribution systems under uncertainty. *Water Resour. Res.* 41(11) W11407.
- Lansey, K.E., EL-Shorbagy, W., Ahmed, I., Araujo, J., and Haan, C. T., 2001. Calibration assessment and data collection for water distribution networks. *J. Hydraul. Eng.* 127(4) 270-279.
- Lansey K.E., 2006. The evolution of optimizing water distribution system applications. 8th Annual Water Distribution Systems Analysis Symposium, Cincinnati, Ohio, USA.
- Lee, B.H., Deininger, R.A. 1992. Optimal locations of monitoring stations in water distribution system. *Journal of Environmental Engineering* (Reston, Va.) 118(1) 4–16.
- Leshno, M., Lin, V.Y., Pinkus, A., Schocken, S., 1993. “Multilayer feed forward networks with a nonpolynomial activation function can approximate any function. *Neural Networks* 6 861–867.
- Lingireddy, S., Ormsbee, L.E., 1998. Neural networks in optimal calibration of water distribution systems. *Artificial neural networks for civil engineers: Advanced features and applications*, I. Flood and N. Kartam, eds., ASCE, Reston, Va., 53–76.
- Loaiciga, H.A., Charbeneau, R.J., Everett, L.G., Fogg, G.E., Hobbs, B.F., Rouhani, S., 1992. Review of ground-water quality monitoring network design. *J. Hydraul. Eng.* 118(1) 11–37.
- Mallick, K.N., Ahmed, I., Tickle, K.S., and Lansey, K. E., 2002. Determining pipe groupings for water distribution networks. *Journal of Water Resources Planning and Management* 128(2), 130–139.
- McKay, M. D., Conover, W. J., and Beckman, R. J. (1979). "A Comparison of Three Methods for Selecting Values of Input Variables in the Analysis of Output from a Computer Code." *Technometrics*, 21(1), 239-245.

- Meier, R.W., Barkdoll, B.D., 2000. Sampling design for network model calibration using genetic algorithms. *Journal of Water Resources Planning and Management* 126(4) 245–250.
- Ormsbee, L.E. 1989. Implicit network calibration. *Journal of Water Resources Planning and Management* 115(2) 243-257.
- Ostfeld, A., Salomons, E., 2004. Optimal layout of early warning detection stations for water distribution systems security. *Journal of Water Resources Planning and Management* 130(5) 377-385.
- Piller, O., Bremond, B., and Morel, P. 1999. A spatial sampling procedure for physical diagnosis in a drinking water supply network. *Proc., Water Industry Systems: Modelling and Optimisation Applications*, Vol. 1, Savic, D.A., Walters, G.A., eds., 309–316, Univ. of Exeter, Exeter, U.K.
- Propato, M., 2006. Contamination warning in water networks: general mixed-integer linear models for sensor location design. *Journal of Water Resources Planning and Management* 132(4) 225-233.
- Rizzo, D.M., Dougherty, D.E., 1996. Design optimization for multiple management period groundwater remediation. *Water Resources Research* 32(8) 2549– 2561.
- Rogers, L.L., Dowla F.U., Johnson, V.M., 1995. Optimal field-scale groundwater remediation using neural networks and the genetic algorithm, *Environmental. Science Technology*, 29 1145–1155.
- Shastri Y., Diwekar, U., 2006. Sensor placement in water networks: A stochastic programming approach . *Journal of Water Resources Planning and Management* 132(3) 192-203.
- Vitkovsky, J.P., Liggett J.A., Simpson, A.R., Lambert, M. F., 2003. Optimal measurement site locations for inverse transient analysis in pipe networks. *Journal of Water Resources Planning and Management* 129(6) 480–492.
- Walski, T.M., 1983. Technique for calibrating network models. *Journal of Water Resources Planning and Management* 109(4) 360–372.

- Walski, T.M., Sharp, W.W., Shields F.D., 1988. Predicting internal roughness in water mains. Miscellaneous Paper EL-88-2, US Army Engineer Waterways Experiment Station, Vicksburg, Miss.
- Yan, S., Minsker, B., 2006. Optimal groundwater remediation design using an adaptive neural network genetic algorithm. *Water Resources Research*, 42(5).
- Yu, G., Powell, R.S., 1994. Optimal design of meter placement in water distribution systems. *International Journal of Systematic Sciences* 25(12) 2155–2166.

LIST OF SYMBOLS USED

a = vector of calibration parameters;

\mathbf{Cov}_a = parameter variance-covariance matrix;

\mathbf{Cov}_z = model prediction variance-covariance matrix;

F_1 = normalized first objective function;

F_2 = normalized second objective function;

f_l = average of model predictions' standard deviation;

$f_{l,ml}$ = Value of f_l assuming that all analyzed locations are monitored;

ITG = Initial training generations;

\mathbf{J} = Jacobian matrix;

\mathbf{J}_{ml} = full Jacobian matrix (all locations monitored);

\mathbf{J}_z = prediction Jacobian matrix;

NF = number of best Pareto (sub)fronts in offspring population;

N_a = number of calibration parameters;

N_k = number of sets of samples from uncertain parameters;

N_l = actual number of measurement devices;

N_l^{\max} = maximum allowed number of measurement devices;

N_l^{\min} = minimum number of measurement devices;

N_{ml} = number of SD potential measurement locations;

N_o = number of measurements in both spatial and temporal domain;

N_z = number of model predictions for whom uncertainty are evaluated;

Superscript T = vector/matrix transpose operator;

s = standard deviation of measurement devices;

y = vector of WDS model predicted variables;

z = vector of model predictions of interest;

LIST OF FIGURES

| | |
|--------------------------------------------------------------------------------------------------------------------|--------------------|
| Figure 1. MOGA-ANN Flowchart | 33 |
| Figure 2. ANN Architecture | 33 |
| Figure 3. Case #1: Anytown Network Layout and Optimal Pressure Logger Locations..... | 34 |
| Figure 4. Case #1: Average Number of Full Model Fitness Evaluations for Different Values of NF and ITG | 34 |
| Figure 5. Case #1: Model Reliability for Different Values of NF and ITG | 35 |
| Figure 6. Case #1: Model reliability for Different Values of NF and the Number of Retraining Data | 35 |
| Figure 7. Case #1: Model Reliability for Different Values of NF and the Number of Hidden Layer Neurons | 36 |
| Figure 8. Case #1: Comparison of the Pareto Optimal Fronts Obtained by the MOGA-ANN and the MCS-based models | 36 |
| Figure 9. Case #1: Comparison of Different Type Fitness Evaluations in MOGA-ANN | 37 |
| Figure 10. Case #2: Skeletonized Mahalat WDS Model and Optimal Pressure Logger Locations... | 37 |
| Figure 11. Case #2: Comparison of Pareto Optimal Fronts Obtained by the MOGA and the MOGA-ANN Models | 38 |
| Figure 12. Case #2: Comparison of Different Fitness Type Evaluations in the MOGA-ANN Model | 38 |

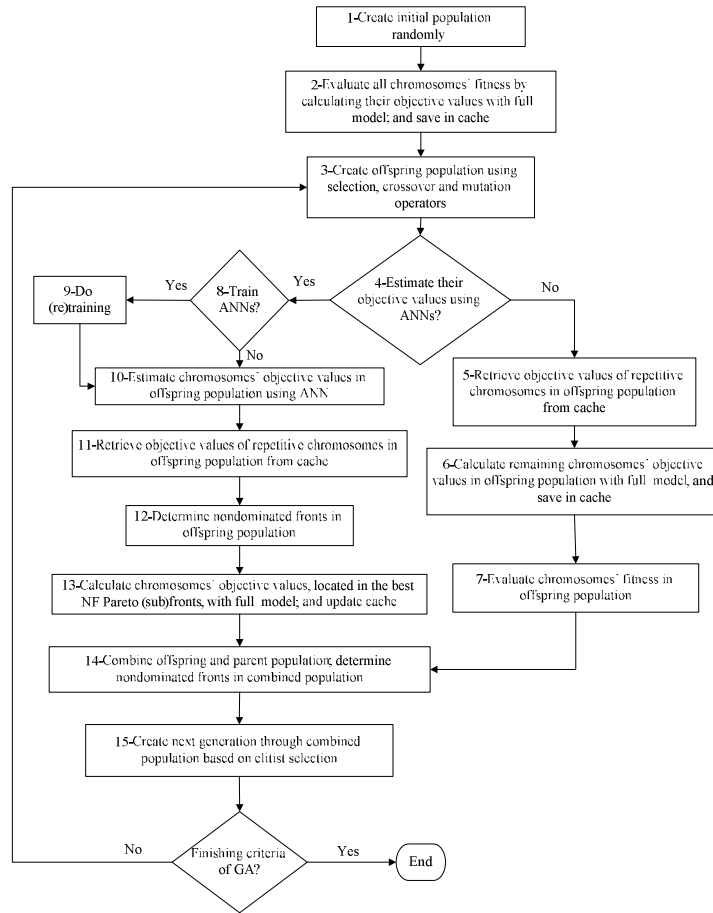


Figure 1. MOGA-ANN Flowchart

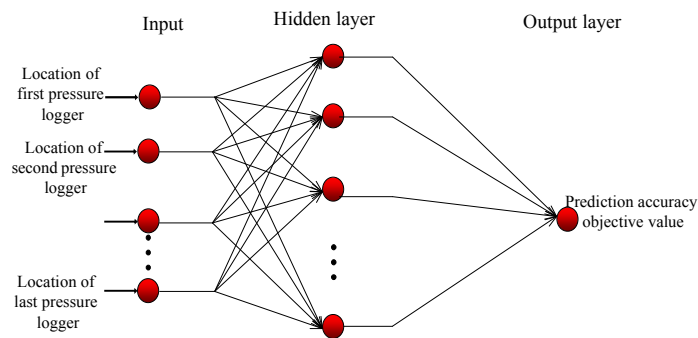


Figure 2. ANN Architecture

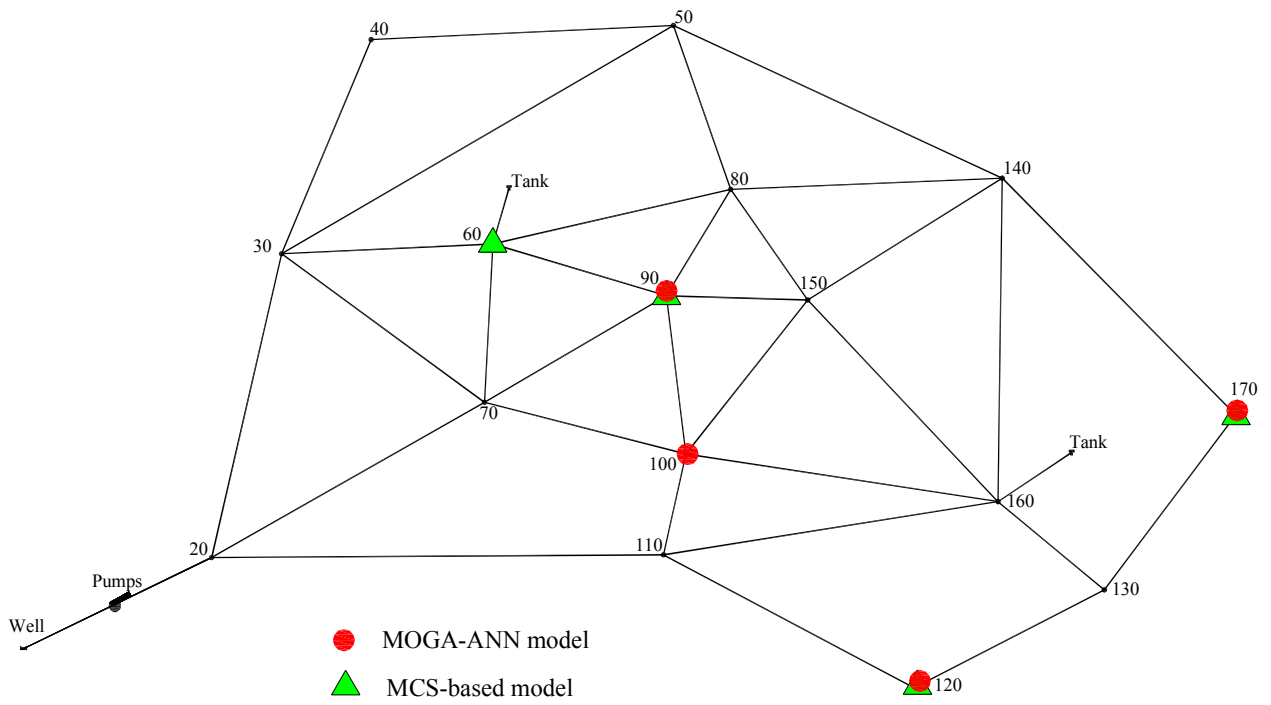


Figure 3. Case #1: Anytown Network Layout and Optimal Pressure Logger Locations

(4 Measurement Points)

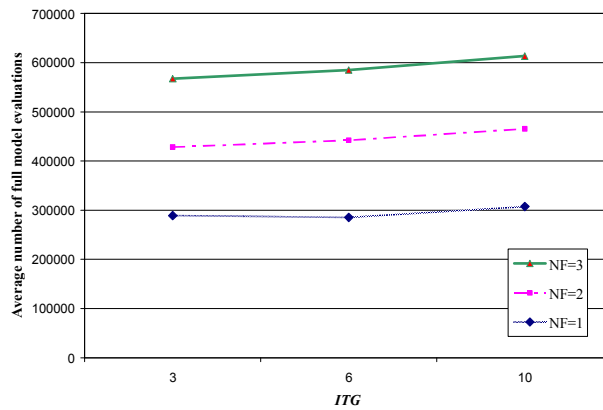


Figure 4. Case #1: Average Number of Full Model Fitness Evaluations for Different Values of NF

and ITG

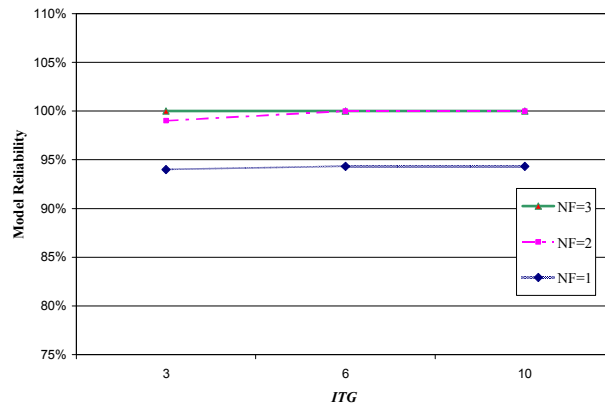


Figure 5. Case #1: Model Reliability for Different Values of NF and ITG

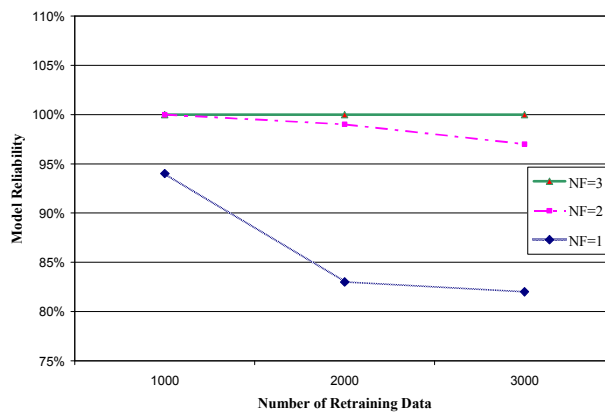


Figure 6. Case #1: Model reliability for Different Values of NF and the Number of Retraining Data

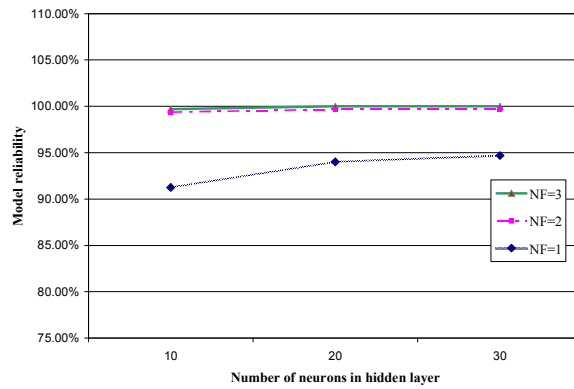


Figure 7. Case #1: Model Reliability for Different Values of NF and the Number of Hidden Layer Neurons

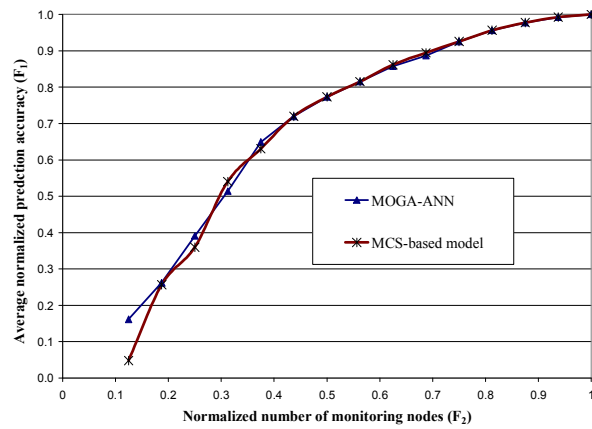


Figure 8. Case #1: Comparison of the Pareto Optimal Fronts Obtained by the MOGA-ANN and the MCS-based models

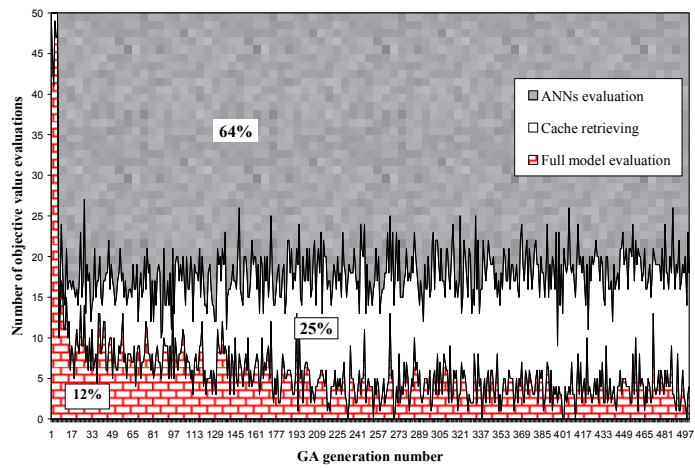


Figure 9. Case #1: Comparison of Different Type Fitness Evaluations in MOGA-ANN

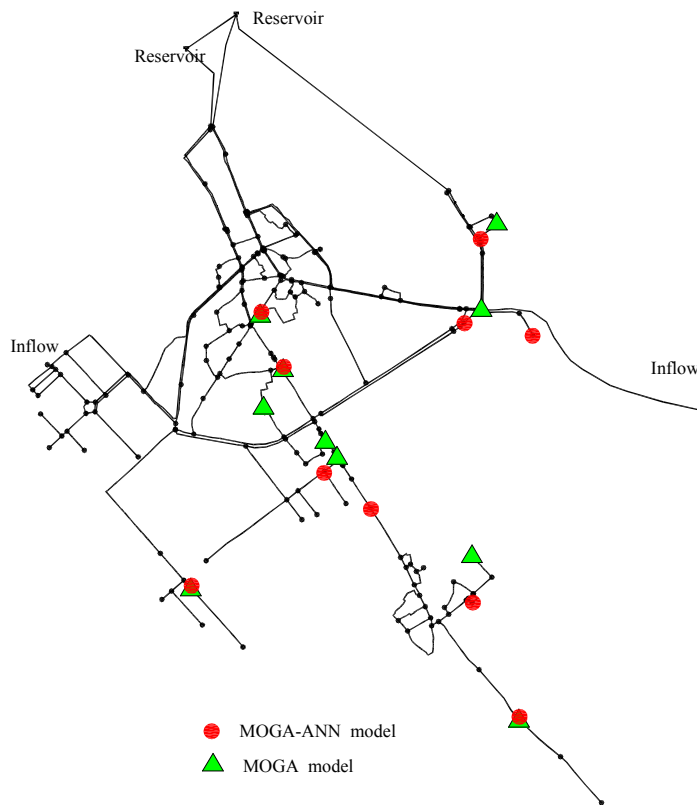


Figure 10. Case #2: Skeletonized Mahalat WDS Model and Optimal Pressure Logger Locations

(10 Measurement Points)

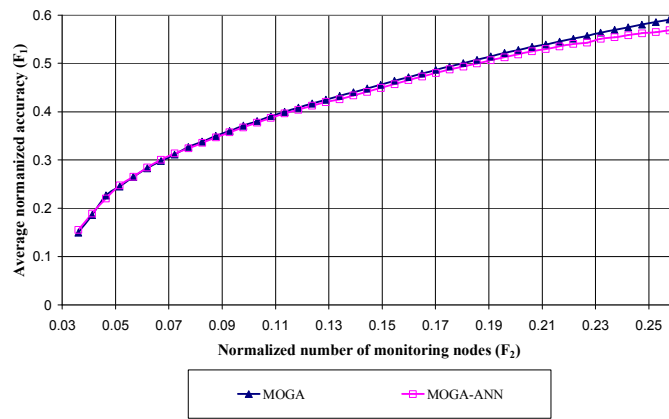


Figure 11. Case #2: Comparison of Pareto Optimal Fronts Obtained by the MOGA and the MOGA-ANN Models

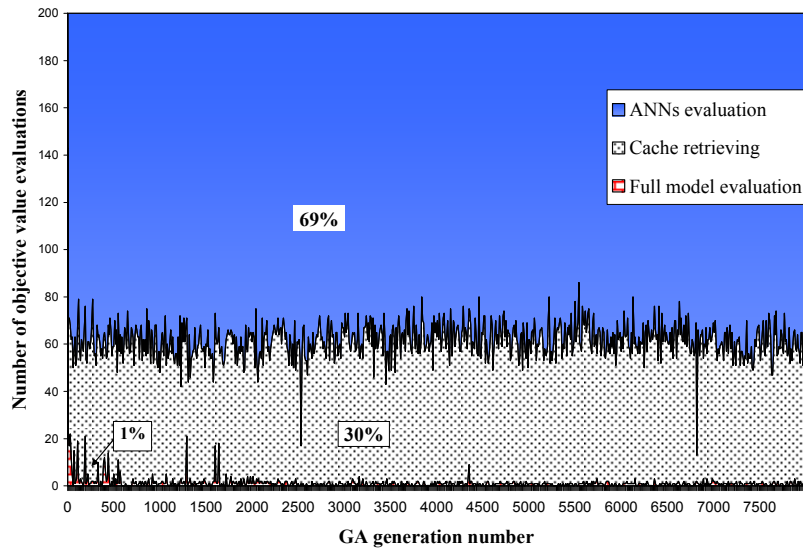


Figure 12. Case #2: Comparison of Different Fitness Type Evaluations in the MOGA-ANN Model

LIST OF TABLES

| | |
|---------------------------------------------------------------------------------------------------------------------------------------------------------------------|----|
| Table 1. Case #1: Pareto Optimal Solutions Obatined by Using the MOGA-ANN and Percentage of Selected Sampling Locations Obatined by Using the MCS-based model | 40 |
| Table 2. Case #1: Statistics of Relative Accuracy for Four Optimal Measurement Locations Obatined by Using the MOGA-ANN and the MCS-based Models | 41 |
| Table 3. Case #1: Comparison of Computational Times | 42 |
| Table 4..Case #2: Summary of Pipe Materials and Diameters..... | 42 |
| Table 5. Case #2: Statistics of Relative Accuracy and Uncertainty for Ten Optimal Measurement Locations Obatined by Using MOGA-ANN and MOGA-ANN..... | 43 |
| Table 6. Case #2: Comparison of the Computational Times Required to Obtain Pareto Optimal Solutions..... | 43 |

Table 1. Case #1: Pareto Optimal Solutions Obtained by Using the MOGA-ANN and Percentage of Selected Sampling Locations Obtained by Using the MCS-based model

| Number of Monitoring Nodes | F2 | F1 | | Node ID | | | | | | | | | | | | | | | |
|----------------------------|--------|--------|----------------|---------|----|-----|-----|-----|-----|-----|-----|-----|-----|-----|-----|-----|-----|-----|-----|
| | | | | 20 | 30 | 40 | 50 | 60 | 70 | 80 | 90 | 100 | 110 | 120 | 130 | 140 | 150 | 160 | 170 |
| 2 | 0.125 | 0.1618 | Opt. locations | 0 | 0 | 0 | 0 | 0 | 0 | 0 | 1 | 0 | 0 | 1 | 0 | 0 | 0 | 0 | 0 |
| | | | Percentage | 0 | 1 | 12 | 10 | 20 | 7 | 6 | 14 | 22 | 0 | 72 | 23 | 3 | 1 | 1 | 3 |
| 3 | 0.1875 | 0.2621 | Opt. locations | 0 | 0 | 0 | 0 | 0 | 0 | 0 | 1 | 1 | 0 | 1 | 0 | 0 | 0 | 0 | 0 |
| | | | Percentage | 0 | 0 | 13 | 6 | 48 | 6 | 5 | 33 | 55 | 13 | 74 | 33 | 3 | 2 | 2 | 10 |
| 4 | 0.25 | 0.3912 | Opt. locations | 0 | 0 | 0 | 0 | 0 | 0 | 0 | 1 | 1 | 0 | 1 | 0 | 0 | 0 | 0 | 1 |
| | | | Percentage | 0 | 0 | 2 | 1 | 46 | 18 | 4 | 75 | 42 | 40 | 87 | 21 | 1 | 3 | 14 | 49 |
| 5 | 0.3125 | 0.5143 | Opt. locations | 0 | 0 | 0 | 0 | 0 | 0 | 0 | 1 | 1 | 1 | 1 | 0 | 0 | 0 | 0 | 1 |
| | | | Percentage | 0 | 0 | 1 | 1 | 63 | 18 | 0 | 95 | 38 | 74 | 95 | 3 | 0 | 1 | 27 | 86 |
| 6 | 0.375 | 0.6491 | Opt. locations | 0 | 0 | 0 | 0 | 1 | 0 | 0 | 1 | 1 | 1 | 1 | 0 | 0 | 0 | 0 | 1 |
| | | | Percentage | 0 | 0 | 5 | 0 | 90 | 28 | 1 | 100 | 43 | 90 | 99 | 0 | 0 | 1 | 50 | 96 |
| 7 | 0.4375 | 0.7198 | Opt. locations | 0 | 0 | 0 | 0 | 1 | 0 | 0 | 1 | 1 | 1 | 1 | 0 | 0 | 0 | 1 | 1 |
| | | | Percentage | 0 | 0 | 14 | 3 | 99 | 45 | 2 | 100 | 49 | 97 | 100 | 1 | 0 | 1 | 93 | 100 |
| 8 | 0.5 | 0.7731 | Opt. locations | 0 | 0 | 0 | 0 | 1 | 1 | 0 | 1 | 1 | 1 | 1 | 0 | 0 | 0 | 1 | 1 |
| | | | Percentage | 1 | 0 | 37 | 8 | 100 | 59 | 8 | 100 | 55 | 99 | 100 | 27 | 3 | 5 | 100 | 100 |
| 9 | 0.5625 | 0.8152 | Opt. locations | 0 | 0 | 0 | 0 | 1 | 1 | 1 | 1 | 1 | 1 | 1 | 0 | 0 | 0 | 1 | 1 |
| | | | Percentage | 2 | 0 | 51 | 16 | 100 | 71 | 21 | 100 | 68 | 99 | 100 | 53 | 4 | 16 | 100 | 100 |
| 10 | 0.625 | 0.8575 | Opt. locations | 0 | 0 | 0 | 0 | 1 | 1 | 1 | 1 | 1 | 1 | 1 | 1 | 0 | 0 | 1 | 1 |
| | | | Percentage | 2 | 0 | 63 | 25 | 100 | 83 | 35 | 100 | 84 | 99 | 100 | 76 | 5 | 30 | 100 | 100 |
| 11 | 0.6875 | 0.8867 | Opt. locations | 0 | 0 | 0 | 0 | 1 | 1 | 1 | 1 | 1 | 1 | 1 | 1 | 0 | 1 | 1 | 1 |
| | | | Percentage | 4 | 0 | 75 | 35 | 100 | 94 | 49 | 100 | 93 | 100 | 100 | 93 | 8 | 50 | 100 | 100 |
| 12 | 0.75 | 0.9257 | Opt. locations | 0 | 0 | 1 | 0 | 1 | 1 | 1 | 1 | 1 | 1 | 1 | 1 | 0 | 1 | 1 | 1 |
| | | | Percentage | 5 | 1 | 87 | 57 | 100 | 98 | 64 | 100 | 97 | 100 | 100 | 100 | 12 | 82 | 100 | 100 |
| 13 | 0.8125 | 0.9561 | Opt. locations | 0 | 0 | 1 | 1 | 1 | 1 | 1 | 1 | 1 | 1 | 1 | 1 | 0 | 1 | 1 | 1 |
| | | | Percentage | 8 | 2 | 96 | 80 | 100 | 99 | 89 | 100 | 100 | 100 | 100 | 100 | 30 | 99 | 100 | 100 |
| 14 | 0.875 | 0.9771 | Opt. locations | 0 | 0 | 1 | 1 | 1 | 1 | 1 | 1 | 1 | 1 | 1 | 1 | 1 | 1 | 1 | 1 |
| | | | Percentage | 10 | 8 | 100 | 96 | 100 | 100 | 100 | 100 | 100 | 100 | 100 | 100 | 88 | 100 | 100 | 100 |
| 15 | 0.9375 | 0.9924 | Opt. locations | 0 | 1 | 1 | 1 | 1 | 1 | 1 | 1 | 1 | 1 | 1 | 1 | 1 | 1 | 1 | 1 |
| | | | Percentage | 19 | 82 | 100 | 100 | 100 | 100 | 100 | 100 | 100 | 100 | 100 | 100 | 100 | 100 | 100 | 100 |

In the “Opt. locations” rows, “1” means pressure logger should be installed in the node and “0” means no pressure logger is required in the node

Table 2. Case #1: Statistics of Relative Accuracy for Four Optimal Measurement Locations

Obtained by Using the MOGA-ANN and the MCS-based Models

| Description | MOGA-ANN | MCS |
|-------------------------------------|----------|--------|
| Mean | 0.3912 | 0.3598 |
| Minimum | 0.1146 | 0.1075 |
| Maximum | 0.5414 | 0.5985 |
| Standard deviation | 0.0499 | 0.0645 |
| 95% confidence interval upper bound | 0.2804 | 0.2387 |
| 95% confidence interval lower bound | 0.4789 | 0.4857 |

Table 3. Case #1: Comparison of Computational Times

| Model type | Computational time (minutes) | The number of deterministic prediction accuracy calculation calls |
|------------|---------------------------------|-------------------------------------------------------------------------|
| MOGA | 32 | 5,000,000 |
| MOGA-ANN | 4 | 590,000 |
| MCS-based | 32 | 5,000,000 |

*The number of deterministic prediction accuracy calculation calls defined by (4) for MOGA and MCS-based model is equal to $N_{pop}N_{gen}N_k$, where N_{pop} is GA population size (50 here) and N_{gen} is the number of GA generation before convergence (500 here) and N_k is the number of samples (200)

Table 4..Case #2: Summary of Pipe Materials and Diameters

| No. | Original Material | Number of Pipes | Diameter (mm) |
|-----|----------------------|--------------------|------------------|
| 1 | Asbestos Cement | 406 | 80-250 |
| 2 | Ductile Iron | 470 | 100-500 |
| 3 | Galvanized Iron | 113 | 25-125 |
| 4 | PVC | 657 | 25-110 |
| 5 | Steel | 166 | 20-65 |

Table 5. Case #2: Statistics of Relative Accuracy and Uncertainty for Ten Optimal Measurement Locations Obtained by Using MOGA-ANN and MOGA-ANN

| Model type | Relative Pressure Prediction Accuracy | | | Pressure Prediction Uncertainty (m) | | |
|------------|---------------------------------------|----------------------|----------------------|-------------------------------------|----------------------|----------------------|
| | Mean | 95% confidence | | Mean | 95% confidence | |
| | | interval lower bound | interval upper bound | | interval lower bound | interval upper bound |
| MOGA | 0.2451 | 0.1836 | 0.2761 | 0.6774 | 0.5838 | 0.9012 |
| MOGA-ANN | 0.2445 | 0.1849 | 0.2747 | 0.6780 | 0.5909 | 0.8919 |

Table 6. Case #2: Comparison of the Computational Times Required to Obtain Pareto Optimal Solutions

| Model type | Computational time (minutes) | The number of deterministic prediction accuracy calculation calls* |
|------------|------------------------------|--------------------------------------------------------------------|
| MOGA | 1,550 | 320,000,000 |
| MOGA-ANN | 65 | 2,098,400 |

*The number of deterministic prediction accuracy calculation calls defined by (4) for MOGA is equal to $N_{pop}N_{gen}N_k$, where N_{pop} is GA population size (200 here) and N_{gen} is the number of GA generation before convergence (8000 here) and N_k is the number of samples (200)